

Examination of gene repertoires and physiological responses to iron and light limitation in Southern Ocean diatoms

Carly M. Moreno¹  · Yajuan Lin² · Sarah Davies¹ · Elaine Monbureau¹ · Nicolas Cassar² · Adrian Marchetti¹

Received: 11 March 2017 / Revised: 12 September 2017 / Accepted: 3 December 2017
© Springer-Verlag GmbH Germany, part of Springer Nature 2017

Abstract

Diatoms play a fundamental role at the base of the polar marine food web. In the Southern Ocean, low iron concentrations and light levels control diatom abundance and distribution. Diatoms must therefore employ strategies that allow them to cope when iron and/or light availability is growth limiting. Through a combination of physiological and molecular-based approaches, we have investigated the physiological response to variable iron concentrations and light levels along with the expressed gene repertoires of nine newly isolated diatoms from the Western Antarctic Peninsula (WAP) region of the Southern Ocean. The diatoms ranged across five orders of magnitude in biovolume and displayed various degrees of susceptibility to low iron and light availability. Under the performed laboratory culture conditions, the growth rates of most diatoms decreased more due to low light level rather than low iron concentrations. Additionally, most diatoms were not subject to further reductions in growth rates when grown under combined low-light and iron-limiting conditions, indicating they are less likely to be co-limited by an additive effect. By sequencing the transcriptomes of these diatoms, we identified genes that likely facilitate their growth under variable iron and light conditions commonly present in the Southern Ocean. Specifically, we investigated the presence of 20 key genes involved in iron acquisition and homeostasis, iron usage in photosynthesis and nitrogen assimilation, and protection from reactive oxygen species. When comparing gene repertoires of recently sequenced transcriptomes of diatoms isolated from around the globe, the prevalence of certain genes exhibited biogeographical patterns that clearly distinguish Southern Ocean diatoms from those isolated from other regions.

Keywords Southern Ocean diatoms · Molecular physiology · Iron limitation · Light limitation · Transcriptomics

Introduction

Phytoplankton, such as diatoms, serve as the base of many polar marine food webs and support a wide variety of Antarctic fauna including krill, fish, penguins, and whales (Saba et al. 2014). Southern Ocean marine ecosystems are being altered by anthropogenic climate change, potentially

resulting in shifts in the composition, diversity, and growth of primary producers. Coastal regions along the Antarctic continent are particularly important as sites of upwelling and elevated primary production (Arrigo et al. 2008). An area of particular concern is the western Antarctic Peninsula (WAP) as it is experiencing rapid changes in climate, ecology, and oceanography (Saba et al. 2014). Biological systems in the WAP are sensitive to ice seasonality, and the recent warming temperatures and decrease in sea ice have resulted in significant decreases in phytoplankton biomass and shifts in species dominance from large diatoms to small flagellated cryptophytes (Montes-Hugo et al. 2009). The phytoplankton communities in these regions are mainly composed of diatoms and prymnesiophytes such as *Phaeocystis*, and are responsible for large fluxes of CO₂ drawdown in the region (Arrigo et al. 2010). However, despite plentiful nitrate and phosphate in the surface waters throughout the Southern Ocean (SO), primary production is often patchy (Moore and Abbott 2000).

Electronic supplementary material The online version of this article (<https://doi.org/10.1007/s00300-017-2228-7>) contains supplementary material, which is available to authorized users.

✉ Adrian Marchetti
amarchetti@unc.edu

¹ Department of Marine Sciences, The University of North Carolina at Chapel Hill, Campus Box 3300, Chapel Hill, NC 27599, USA

² Division of Earth and Ocean Sciences, Nicholas School of the Environment, Duke University, Durham, NC 27708, USA

Two primary resources, iron and light, can limit the growth of phytoplankton in the Southern Ocean (Sunda and Huntsman 1997; Boyd et al. 2007; Strzepek et al. 2012). Iron is supplied naturally to the Southern Ocean by aeolian deposition, melting of sea ice, resuspension of sediments, and deep winter mixing; however, rapid biological uptake and particle scavenging deplete available iron and create high-nutrient (N and P), low-chlorophyll (HNLC) conditions in which primary productivity is seasonally limited by iron availability (Martin 1990; Edwards et al. 2001; Cassar et al. 2007). Strong evidence for iron limitation comes from the results of iron fertilization experiments and natural iron inputs, both of which have resulted in massive phytoplankton blooms where diatoms are the main responders (Boyd et al. 2000; Blain et al. 2007; Smetacek et al. 2012).

Most diatoms have higher growth requirements for external iron (and other nutrients) relative to other types of phytoplankton due to a combination of their larger sizes and higher maximum growth rates (Raven 1990; Raven et al. 1999). Iron limitation in diatoms results in decreased growth rate, chlorophyll-*a* content, and photosynthetic efficiency (Sunda and Huntsman 1995; Timmermans et al. 2001; Arrigo et al. 2010). Diatoms can acclimate and adapt to low-iron conditions in a number of ways, including reducing cellular iron-to-carbon ratios (Sunda and Huntsman 1995; Strzepek et al. 2012), altering photosynthetic architecture (Strzepek and Harrison 2004), substituting iron-containing redox catalysts with non-iron-containing proteins or those that use other metal cofactors (La Roche et al. 1996; Peers and Price 2006), activating a high-affinity iron uptake system (Maldonado et al. 2006), performing luxury uptake of iron (Marchetti et al. 2009), and increasing surface area-to-volume (SA:V) ratios through changes in their size and shape (Sunda and Huntsman 1995; Marchetti and Harrison 2007).

Light availability is another important seasonal driver of phytoplankton growth and the determinant in occurrence of blooms. Deep winter mixed layers (> 100 m), and months of darkness, can result in phytoplankton experiencing considerable periods of light limitation (Sallée et al. 2010). Climate change is predicted to affect light availability and iron supply in the Southern Ocean (Feng et al. 2010; Smith et al. 2014), with both positive and negative effects on phytoplankton growth and primary productivity, particularly in the WAP (Montes-Hugo et al. 2009; Saba et al. 2014). In the northern region of the WAP, declines in sea ice and increased winds have resulted in deeper mixed layers with an overall decrease in mean light levels, causing significant declines in summertime surface chlorophyll concentrations (Venables et al. 2013). In the southern region of the WAP, there is an increase in surface chlorophyll concentrations due to sea ice melt and increased stratification (Montes-Hugo et al. 2009). While increased irradiance is the sole controlling factor in initiating blooms in spring and early summer,

by mid-summer iron can be the main factor limiting primary production due to shoaling of the mixed layer (Boyd et al. 2001). However, sea/ice dynamics are complicated especially in light of a warming climate. In future scenarios, decreased stratification from stronger winds might lead to alleviated seasonal nutrient (iron) limitation, as nutrient-rich deep water would be mixed to the surface more frequently. Conversely, iron limitation might become more pronounced as sea ice and glacial melt strengthens stratification, although this would reduce the variability in light conditions (Venables et al. 2013). However, co-limitation of iron and light is also possible at different times and regions of the Southern Ocean (Sunda and Huntsman 1997; Boyd 2002).

Numerous studies have examined the unique physiological responses of single to a few SO diatoms to iron and light limitation (e.g., Arrigo et al. 2010; Alderkamp et al. 2012; Strzepek et al. 2012). However, a thorough assessment of the extent to which SO diatoms can cope under low-iron and low-light conditions along with the molecular underpinnings orchestrating these responses is still lacking. In an effort to expand on the findings of previous studies, we compared the physiology of nine newly isolated SO diatoms grown under a matrix of iron and light conditions, in conjunction with a transcriptomic investigation into the presence of iron and light-related genes and metabolic pathways of each diatom. Some of the examined genes have been shown to have a direct role in iron homeostasis, photosynthesis, and nitrogen assimilation, while others have putative functions in other pathways affected by iron and/or light. In addition, we utilized publically available transcriptomes from the Marine Microbial Eukaryote Transcriptome Project (MMETSP; Keeling et al. 2014) to provide insights into the molecular bases of physiological adaptations to low-iron and low-light conditions in diatoms isolated from the Southern Ocean compared with non-Southern Ocean diatoms from regions around the globe.

Materials and methods

Diatom isolation and identification

Nine species of diatoms were isolated from the Western Antarctic Peninsula along the Palmer LTER sampling grid in 2013 and 2014 (Table 1). Isolations were performed using an Olympus CKX41 inverted microscope by single cell isolation with a micropipette (MacIntyre and Cullen 2005). Diatom species were identified by morphological characterization and 18S rRNA gene (rDNA) sequencing. DNA was extracted with the DNeasy Plant Mini Kit according to the manufacturer's protocols (Qiagen). Amplification of the nuclear 18S rDNA region was achieved with standard PCR protocols using

Table 1 List of SO diatom isolates with strain designation, isolation location along the PalmerLTER cruise track, best hit to 18S rDNA sequence in NCBI GenBank including sequence similarity, and 18S rDNA GenBank accession number

Polar diatoms	Strain ID	PalmerLTER station	Latitude	Longitude	GenBank best hit	% similarity to best hit	Accession number
<i>Thalassiosira antarctica</i>	UNC1404	200.180	– 66.579	– 72.739	DQ514874.1	99	KX253953
<i>Navicula</i> sp.	UNC1405	100.040	– 68.112	– 72.346	KC771158.1	99	KX253954
<i>Chaetoceros</i> cf. <i>sociales</i>	UNC1406	200.–020	– 67.296	– 69.665	HM581778.1	100	KX253957
<i>Chaetoceros rostratus</i>	UNC1407	200.–020	– 67.296	– 69.665	X85391.1	99	KX253958
<i>Proboscia alata</i>	UNC1408	200.040	– 67.511	– 70.589	AY485525.1	99	KX253955
<i>Pseudo-nitzschia subcurvata</i>	UNC1409	200.040	– 67.511	– 70.589	AY485490.1	99	KX253952
<i>Actinocyclus actinochilus</i>	UNC1410	400.040	– 66.254	– 67.337	AY485506.1	99	KX253959
<i>Eucampia antarctica</i>	UNC1411	200.020	– 67.642	– 70.269	X85389.1	98	KX253956
<i>Fragilariopsis cylindrus</i>	UNC1301	200.180	– 66.579	– 72.739	AY485467	100	–

eukaryotic-specific, universal 18S rDNA forward and reverse primers. Primer sequences were obtained from Medlin et al. (1988) and are as follows: 18AF 5'-AAC CTGGTTGATCCTGCCAGT-3' and 18BR 5'-TGATCC TTCTGCAGGTTACCTAC-3'. The amplified region was between 1764 and 1803 base pairs (bp) for all diatoms, except *Navicula* sp. and *C. cf. sociales*, for which the 18S rDNA regions were 1660 and 1627 bp, respectively.

Pseudo-nitzschia species are often difficult to identify by their 18S rDNA sequence; therefore, additional confirmation of the taxonomic identification of *P. subcurvata* was provided through sequencing of an 18S-ITS1-5.8S region. Amplification of this region was performed with the 18SF-euk and 5.8SR-euk primers of Hubbard et al. (2008): 18SF-euk 5'-CTTATCATTTAGAGGAAGGTG AAGTCG-3' and 5.8SR-euk 5'-CTGCGTTCTTCATCG TTGTGG-3'. Analysis of this ITS1 fragment resulted in the highest sequence homology and length similarity to *P. subcurvata* (Strain: 1-F, Accession number: DQ329205). PCR products were purified using either QIAquick PCR Purification Kit (Qiagen) or ExoSAP-IT (Affymetrix) and sequenced by Sanger DNA sequencing (Genewiz). Sequences were edited using Geneious Pro 5.6.4 software (Kearse et al. 2012) and BLASTn sequence homology searches were performed against the NCBI nucleotide non-redundant (nr) database to determine species with a cutoff identity of 98% (Altschul et al. 1990).

Diatom phylogenetic tree analysis was performed with Geneious Pro 5.6.4 and included 75 diatom 18S rDNA sequences from publically available genomes and transcriptomes, including those in the MMETSP database. Diatom sequences were trimmed to the same length (1297 bp) and aligned with MUSCLE (Edgar 2004). A phylogenetic tree was created in Mega v.6 with the Maximum-likelihood method of tree reconstruction, the Jukes-Cantor genetic distance model, and 100 bootstrap replicates (Jukes and Cantor 1969).

Growth conditions, physiological characteristics, and biovolumes

Isolates were maintained at 4 °C in constant irradiance at intensities of either 10 $\mu\text{mol photons m}^{-2} \text{s}^{-1}$ (low light) or 90 $\mu\text{mol photons m}^{-2} \text{s}^{-1}$ (growth-saturating light) and with media containing high and low iron concentrations. Light intensities were chosen based on previous published culture experiments (Arrigo et al. 2010; Strzepek et al. 2011; Petrou et al. 2014; Hoppe et al. 2015). Isolates were grown in a matrix of Fe and light intensities: high-iron, growth-saturating light (+FeSL), low-iron, growth-saturating light (–FeSL), high-iron, low-light (+FeLL), and low-iron, low-light (–FeLL) conditions. Cultures were grown in the synthetic seawater medium, AQUIL, enriched with filter sterilized vitamins and trace metals containing 100 $\mu\text{mol L}^{-1}$ EDTA. The growth media also contained 300 $\mu\text{mol L}^{-1}$ nitrate, 200 $\mu\text{mol L}^{-1}$ silicic acid, and 20 $\mu\text{mol L}^{-1}$ phosphate. Fe bound to EDTA was added for total iron concentrations of either 1370 or 3.1 nmol L^{-1} to achieve high-iron and low-iron media, respectively, in the presence of 100 $\mu\text{mol L}^{-1}$ EDTA. Predicted dissolved inorganic iron (Fe²⁺) concentrations are $\sim 2.7 \times 10^3 \text{ pmol L}^{-1}$ for the high-iron and $\sim 6 \text{ pmol L}^{-1}$ for the low-iron treatments, although these may deviate slightly due to the lower culturing temperature and light intensities used in our experiments (Marchetti et al. 2009). All cells were pre-acclimated to each treatment's light level and iron concentration for at least three transfers before reported growth rates or photophysiology measurements were collected. All media preparation and subsampling were performed under a positive-pressure, trace metal clean laminar flow hood. Cultures were grown in acid-washed 28-mL polycarbonate centrifuge tubes (Nalgene) and maintained in exponential phase by dilution. When cells were in late-exponential phase, 50–1000 μL of dense culture media was transferred into 28 mL of fresh media resulting in a dilution factor between 29 and 560. Specific growth

rates of successive transfers were calculated from the linear regression of the natural log of in vivo chlorophyll-a fluorescence using a Turner 10-AU fluorometer (Brand et al. 1981). Interactive effects between iron and light were determined by performing a two-way ANOVA. Post hoc Tukey tests were also performed in order to determine which treatments differed significantly ($p < 0.05$) ($n \geq 3$). All tests passed the Shapiro–Wilks Normality test unless otherwise stated, in which case p values are representative of the Mann–Whitney Rank Sum test. ANOVA did not test the interaction between +FeSL and –FeLL, and therefore we performed an unpaired t test between these treatments for significant differences in growth rate and photophysiological parameters. In the case of *T. antarctica*, no growth rates were measured in the combined low-iron and low-light conditions as cultures did not achieve steady-state growth in this treatment. Statistical analyses of growth rates and photophysiological data were performed with SigmaPlot 12.5 (SysStat Software Inc.). Plots were created using Matlab R2014b software.

Photophysiological parameters were measured with a Fluorescence Induction Relaxation System (FIRE) (Satatlantic). Samples were dark acclimated for at least 10 min and measurements were taken of each culture for photosynthetic efficiency ($F_v:F_m$), and functional absorption cross section of PSII (σPSII [$\text{\AA}^2 \text{ quanta}^{-1}$]). $F_v:F_m$ and σPSII were measured when cultures were in mid- to late-exponential phase. FIRE parameters were set to measure single-turnover flash of PSII reaction centers (single closure event) with a sample delay of 100 and a total of 50 iterations (Gorbunov and Falkowski 2005).

To estimate biovolumes of each diatom species, frustules were viewed using an Olympus BX61 Upright Wide Field Microscope with the differential interference contrast imaging mode and a 60X/1.42 Oil PlanApo N objective lens. Valve apical length (AL), transapical width (TW), and perivalvar height (PH) dimensions were estimated with Scion Image software (<http://scion-image.software.informer.com>; June 2015). Mean diatom biovolumes were calculated according to Hillebrand et al. (1999) where pennate diatoms were modeled after elliptic prisms and centric diatoms were modeled after cylinders. For all species except *T. antarctica*, at least four cells were imaged and measured to obtain average cell dimensions (*T. antarctica* sample size $n = 1$).

RNA extractions, transcriptome library preparation, and sequencing

Cultures for high-throughput sequencing of mRNA were grown in acid-washed 2L polycarbonate bottles in iron-replete conditions under growth-saturating light ($90 \mu\text{mol photons m}^{-2} \text{ s}^{-1}$) in order to achieve enough RNA material for subsequent sequencing. After reaching late-exponential/early-stationary phase, cultures were harvested onto

polycarbonate filters (3.0 μm pore size, 25 mm) and stored at -80°C . Glass beads were added to the cells before they were mechanically disrupted for 1 min in a bead beater. Further RNA isolation steps were performed according to the RNAqueous 4PCR Kit (Ambion) protocol. Residual genomic DNA was eliminated by DNaseI digestion at 37°C for 45 min. Sample concentrations were quantified using a Qubit 2000 Fluorometer. An Agilent Bioanalyzer 2100 was used to determine RNA integrity. mRNA libraries were generated with $\sim 2 \mu\text{g}$ of total RNA and prepared with the Illumina TruSeq Stranded mRNA Library Preparation Kit. Samples were individually barcoded and pooled prior to sequencing on the Illumina MiSeq platform at the High-Throughput Sequencing Facility (HTSF) at UNC-Chapel Hill. Sequencing resulted in approximately 0.7–2 million paired-end reads of 2×300 bp per sample (Table 2).

Sequence assembly and annotation

Illumina TruSeq adapters and poly-A tails were trimmed from raw reads using the Fastx_toolkit v0.0.13 clipper function. Fastq_quality_filter was used to remove poor-quality sequences, such that remaining sequences had a minimum quality score of 20 with a minimum of 80% of bases within a read meeting this quality score requirement. Any remaining raw sequences less than 50 base pairs in length were also removed. Merged files were assembled de novo using Trinity 2.0.6 (Grabherr et al. 2011). The resulting assembly was filtered to remove contigs less than 200 bp in length. Trinity-generated components (a group of contigs representing possible splice variants of the same gene) were then used for sequence homology searches (BLASTx E-value $\leq 10^{-5}$) against the Kyoto Encyclopedia of Genes and Genomes (KEGG) database (Kanehisa et al. 2006).

To assess the quality of our Trinity-assembled transcriptomes and annotation, protein-coding sequences were used to determine completeness and contiguity. BUSCO v.2 (Benchmarking Universal Single-Copy Orthologs) software was used to assess the completeness of genomes and transcriptomes based on sets of single-copy orthologous groups derived from OrthoDB that are highly conserved within multiple lineages (Simão et al. 2015). Completeness was assessed by using the eukaryote BUSCO gene set, which contains 303 genes, to recover orthologs within our transcriptomes. Completed, duplicated, and fragmented orthologs were determined by meeting an ‘expected score’ and having aligned sequences within two standard deviations of the BUSCO gene’s length. Duplicated orthologs are those that have multiple copies of full-length genes that meet the ‘expected score’ and length cutoffs of the BUSCO gene. A second metric of completeness was performed by evaluating conserved pathways, such as the ribosome and spliceosome, using the single-directional best-hit method in the KEGG

Table 2 Statistics of sequencing, assembly, annotation, and quality metrics for completeness and contiguity for the SO diatom transcriptomes

	<i>Eucampia antarctica</i>	<i>Chaetoceros cf. sociales</i>	<i>Proboscia alata</i>	<i>Actinocyclus actinochilus</i>	<i>Navicula</i> sp.	<i>Thalassiosira antarctica</i>	<i>Chaetoceros rostratus</i>	<i>Pseudonitzschia subcurvata</i>
Raw sequence reads	2,127,016	1,186,729	994,652	1,156,014	678,857	1,360,375	1,947,526	1,029,044
Number of contigs	7017	13,951	35,446	46,996	50,365	51,335	43,335	30,791
Number of isogroups	6834	13,825	34,393	44,018	48,609	47,947	39,811	28,995
Transcriptome size (Mb)	2.3	4.9	15.2	24.7	26.6	29.1	27	27.1
Average contig length (bp)	330	353	430	526	527	567	624	881
Maximum contig length (bp)	6103	5810	7209	5975	7283	6551	6817	8191
Minimum contig length (bp)	224	200	200	200	200	200	200	200
N50	327	351	465	638	622	736	851	1265
Contiguity ^a	0.1	0.07	0.11	0.2	0.16	0.23	0.19	0.25
BUSCO ^b (%)	16	34	42	65	62	71	69	74
KAAS pathway completeness								
Spliceosome (%)	21	32	64	87	65	75	77	79
Ribosome (%)	60	73	80	70	80	81	79	70
KEGG—functionally annotated contigs	2158 [0.22]	2473 [0.24]	4098 [0.16]	4571 [0.13]	5226 [0.12]	4935 [0.15]	4845 [0.15]	4568 [0.16]

^aThreshold 0.75^bCompleteness of genome based on 303 core eukaryotic genes

Automatic Annotation Server (KAAS) (Moriya et al. 2007). Finally contiguity, or the distribution of longest-assembled contigs mapped to reference genes, was calculated at the 0.75 level according to Martin and Wang (2011) with custom scripts.

To obtain raw count data for each transcriptome, unassembled sequence reads were aligned to the final Trinity assembly using Bowtie 2 v2.2.5, with the end-to-end option and the R and D parameters set to 10 and 20, respectively (Langmead and Salzberg 2012). Only unique read pairs that aligned once were reported. The resulting count data correspond to the number of unique read matches per Trinity component. Mapped reads were normalized by the Reads per Kilobase per Million reads method (RPKM) (Mortazavi et al. 2008). RPKM takes into consideration two biases from Illumina sequencing runs: library size and gene length; however, it has been shown that normalizing gene expression by gene length can introduce a bias toward less expressed genes (Oshlack and Wakefield 2009). While RPKM has been shown to be inconsistent between samples, as the expressed transcript length can vary between samples, it is still a useful unit as a semi-quantitative measure for identifying presence

and relative abundance of key genes of interest in this study (Li et al. 2009).

Gene presence biogeographical distribution

Twenty salient protein-encoding genes of interest were selected in the study to investigate the molecular basis of iron and light limitation in polar diatoms (Online Resource 1). These genes include ferritin (*FTN*), iron-starvation-induced protein -1, -2a, and -3 (*ISIP1*, *ISIP2a* and *ISIP3*), flavodoxin (*FLDA*), ferredoxin (*petF*), plastocyanin (*PCYN*), cytochrome *c*₆ (*CYTC6*), Fe-superoxide dismutase (*SOD*), mitochondrial alternative oxidase (*AOX*), multi-copper oxidase (*MCO*), iron (III) permease (*FTR1*), ferric reductase (*FRE*), rhodopsin (*RHO*), plastid terminal oxidase (*PTOX*), cellular repressor of EA1-stimulated genes (*CREG*), natural resistance-associated macrophage protein (NRAMP), nitrite and nitrate reductase (*NiR*, *NR*), and argininosuccinate synthase (*ASSY*). Reference sequences for each of these genes were obtained from the *F. cylindrus* and *P. tricorutum* JGI genome portals and *T. pseudonana* and *T. oceanica* NCBI and GenBank repositories (Online Resource 1; Bowler et al.

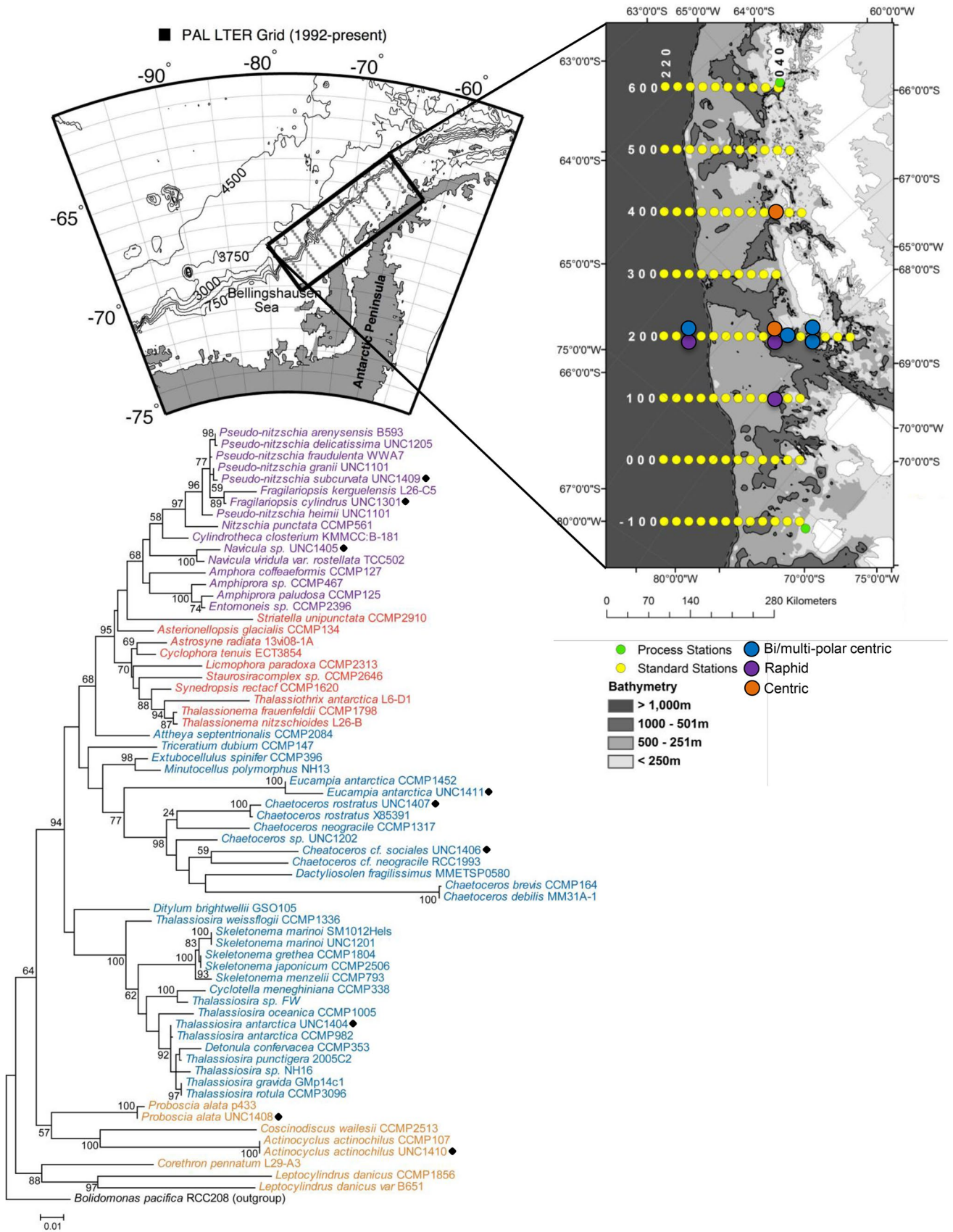


Fig. 1 Map of the Pal-LTER study region and sampling grid (Courtesy R. Iannuzzi and D. Martinson), modified from <http://pal.lternet.edu/gallery/index.php/envira/palmer-maps/>. Yellow circles denote LTER grid stations and green circles denote process stations. Other circles denote stations where isolates were collected and are colored based on diatom clade. Stations are 20 km apart on lines 100 km apart. The shading indicates bathymetry. Phylogenetic tree generated through Maximum-likelihood analysis of 18S rDNA of diatoms sequenced as part of the MMETSP and diatom isolates from this study (denoted with a black diamond). Best hit to 18S rDNA sequences in NCBI GenBank is also included for each isolate. Colors distinguish bi-polar (blue) and radial (orange) centric diatoms and raphid (purple) and araphid (red) pennate diatoms. Node labels show > 50% consensus support for tree arrangement. *Bolidomonas pacifica*, a eukaryotic, picoplanktonic heterokont was used as the out-group

2008; Mock et al. 2017). Reference sequences were identified in the transcriptomes by translated nucleotide homology searches (tBLASTn) with an e-value cutoff of $< 10^{-5}$. A reciprocal tBLASTn homology search was performed for each transcriptome against the KEGG GENES database, using the single-directional best-hit method KAAS online tool to ensure consistent gene annotations (Moriya et al. 2007). The RPKM unit was determined for Trinity-generated components that were homologous with the reference query. We calculated RPKM as a way to semi-quantitatively confirm likelihood of the presence of a gene, assuming that genes with high transcript abundance are more likely to be detected, if present (Online Resource 1). Although a number of these genes have been shown to have increased expression under iron-limiting growth conditions, transcripts are also present within Fe-replete cells (Kustka et al. 2007; Allen et al. 2008; Lommer et al. 2012). Transcripts for each gene detected in our isolates were translated and aligned using Geneious 5.6.4 (Online Resource 2). Included in these alignments are BLASTp sequences for genes of interest from several MMETSP transcriptomes from the same diatom species (different strains), where available.

Subsequently, reference sequences were identified in the MMETSP protein database by BLASTp (E -value $< 10^{-5}$) homology searches among the diatom transcriptomes. The 76 diatoms sequenced as part of the MMETSP include raphid and araphid pennates, and radial and bi-multipolar centrics isolated from all ocean basins including coastal, open-ocean, polar, temperate, tropical, and HNLC regions. The transcriptomes and their associated latitude and longitude were obtained from iMicrobe Data Commons (Project Code CAM_P_0001000) and the National Center for Marine Algae and Microbiota (NCMA) (Online Resource 1). Quantitative read counts, through RPKM or other differential analysis, could not be used for comparing genes between samples because of inherent differences in culturing conditions and sequencing methods. Therefore, we made a semi-quantitative comparison by investigating the

presence or absence of genes within the MMETSP database. Importantly, because gene expression as well as transcriptome depth varies among cultures and growth conditions, the absence of a gene could perhaps be due to insufficient sequencing depth and/or transcriptional regulation. Thus, our survey provides evidence of presence, but not definitive absence from the genome.

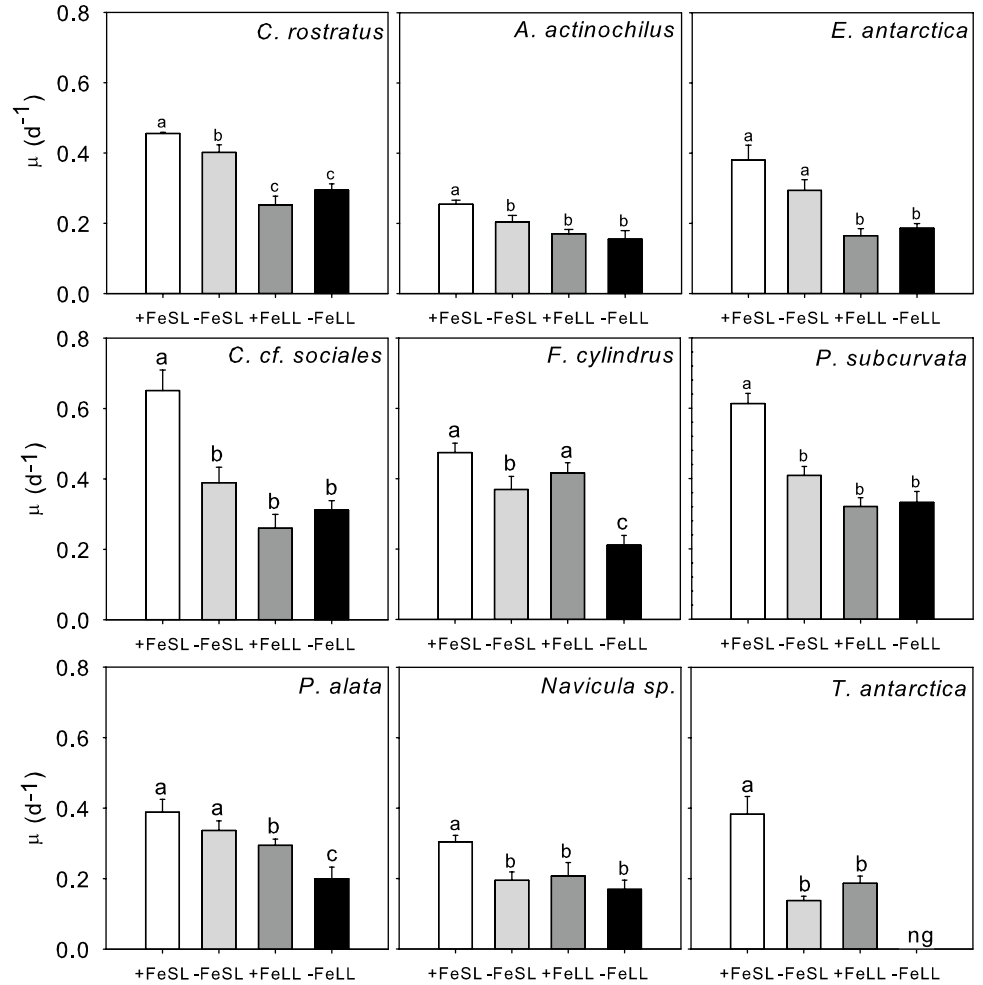
To understand if these diatom genes had a biogeographical distribution throughout global ocean surface waters, we performed sequence homology searches of our genes of interest in the MMETSP database, as well as the transcriptomes of two pennate diatoms isolated from iron-limited waters in the NE Pacific Ocean (*P. granii* and *Grammonema cf. islandica*) and the genome of *F. cylindrus* (Online Resource 1). In total, 65 diatom species were isolated in regions outside of the Southern Ocean, while 22 species were isolated in the vicinity of the Southern Ocean (arbitrarily defined as the area south of 47°S). Custom Matlab scripts allowed global biogeographical distribution of key genes of interest to be mapped by their isolation location. Fisher's exact test was used to compare the distribution of genes that were present or absent in diatoms isolated from Southern Ocean compared to non-Southern Ocean regions.

Results

Isolates collected for this study include three raphid pennate diatoms: *Pseudo-nitzschia subcurvata*, *Fragilariopsis cylindrus* and a *Navicula* sp.; two radial centric diatoms: *Actinocyclus actinochilus* and *Proboscia alata*; and four bi-multipolar centrics: *Thalassiosira antarctica*, *Eucampia antarctica*, *Chaetoceros cf. sociales* and *Chaetoceros rostratus*. Our diatom collection did not include any araphid pennates. The diatoms were isolated from the following Pal-LTER stations: 200.–020 in Marguerite Bay; 200.180, an off-shelf region; and 400.040, 200.040, and 100.040 in mid-shelf regions (Table 1). Full-length 18S rDNA sequences were aligned with 76 other diatom 18S rDNA sequences obtained from the MMETSP database (Fig. 1). Despite originating from a relatively small geographic region, these diatoms represent diverse lineages. Of the diatom transcriptomes sequenced as part of the MMETSP, five of our polar isolate transcriptomes are unique—the transcriptomes of *A. actinochilus*, *Navicula* sp., *P. subcurvata*, *C. rostratus*, and *C. cf. sociales* have not been previously sequenced.

We investigated growth and photophysiology under two different iron and light conditions. Among the isolates grown in iron-replete, growth-saturating light conditions (+FeSL), maximum growth rates ranged from 0.25 d⁻¹ for *A. actinochilus* to 0.65 d⁻¹ for *C. cf. sociales* (Fig. 2); $F_v:F_m$ values ranged from 0.47 for *E. antarctica* to 0.55 for *C. cf. sociales*; and σ_{PSII} ranged from 222 for *T. antarctica*

Fig. 2 Comparison of growth rates for the nine diatom isolates grown under high-iron, growth-saturating light (+FeSL), low-iron, growth-saturating light (−FeSL), high-iron, low-light (+FeLL), and low-iron, low-light (−FeLL) conditions. See methods for details of specific treatments. Letters denote significant differences in growth rates (ANOVA, $p < 0.05$; Student's t test or Mann–Whitney, $p < 0.05$). Error bars represent one standard error of the mean ($n \geq 3$). ng signifies no growth in a treatment



to $511 \text{ \AA}^2 \text{ quanta}^{-1}$ for *F. cylindrus* (Online Resource 2). Maximum specific growth rates under iron-replete conditions determined for *F. cylindrus*, *E. antarctica*, *P. alata*, *T. antarctica*, and *A. actinochilus* are comparable to previously published growth rates of the same or closely related polar species (Agusti and Duarte 2000; Timmermans et al. 2004; Strzepek et al. 2012).

The growth rates of isolates in low-iron, saturating light conditions (−FeSL) were reduced by 12–64% compared to +FeSL (Fig. 2 and Online Resource 2). All diatoms, except *P. alata* and *E. antarctica*, experienced iron limitation under our low-iron conditions, as their growth rates were significantly reduced (ANOVA, $p < 0.05$). In iron-limited cells, $F_v:F_m$ is expected to decline as excitation energy is less efficiently transferred from the light-harvesting antenna systems to PSII reaction centers (Schrader et al. 2011). This reduced efficiency is supported by previous research in culture and field-based experiments (Greene et al. 1991; Suggett et al. 2009; Petrou et al. 2014). In our study, $F_v:F_m$ was generally less responsive to iron stress than was growth rate. For *Navicula sp.*, *T. antarctica*, and *C. cf. sociales*, $F_v:F_m$ decreased significantly from 19 to 49% (ANOVA, $p < 0.05$)

relative to the maximum $F_v:F_m$ in the +FeSL culture, but for the other species there were no significant changes (Online Resource 2). Conversely, σ_{PSII} characteristically increases under iron-limited conditions as a result of an increase in the ratio of PSII antenna complexes relative to reaction center complexes (Greene et al. 1991). The increase in σ_{PSII} has also been proposed to be due to an increase in the size of the absorption cross-section area, rather than the number of the photosynthetic subunits (Strzepek et al. 2012), which might also facilitate healthier photosystems in low light. In our study, σ_{PSII} was observed to significantly increase (ANOVA, $p < 0.05$) under low-iron conditions in five of the eight species, including *F. cylindrus*, *Navicula sp.*, *T. antarctica*, *E. antarctica*, and *C. cf. sociales*. *P. alata* did not exhibit any characteristics associated with iron limitation. While a decrease in growth rate and $F_v:F_m$ was not observed in *E. antarctica*, there was an increase in σ_{PSII} , perhaps suggesting this species was experiencing the onset of iron-stressed growth when grown under our low-iron conditions.

A decrease in light intensity from 90 to 10 $\mu\text{mol photons m}^{-2} \text{ s}^{-1}$ in the high-iron cultures (+FeLL) significantly decreased the specific growth rate by 12–60% for all

diatoms, except *F. cylindrus* ($p < 0.05$; Online Resource 2). *F. cylindrus* was the only diatom not to express decreased growth in the iron-replete, low-light treatment, which may be due to its photoacclimatory abilities. Growth-saturating irradiance for *F. cylindrus* is as low as $25 \mu\text{mol photons m}^{-2} \text{s}^{-1}$, but has been shown to photoacclimate to irradiances as high as 250 (Kropuenske et al. 2009; Arrigo et al. 2010). In the low-light cultures, $F_v:F_m$ either remained the same or increased, and for *A. actinochilus*, *P. subcurvata*, *E. antarctica*, and *C. rostratus*, the increase was statistically significant ($p < 0.05$). There was no significant change in σ_{PSII} in any of the +FeLL cultures compared to +FeSL cultures. These trends in $F_v:F_m$ and σ_{PSII} suggest SO diatoms might have unique mechanisms to maintain an efficient photochemical yield and cross-sectional adsorption area of PSII, despite a reduction in growth under low-light conditions. Interestingly, when diatoms overwinter in the Southern Ocean, experiencing months of almost complete darkness, they retain a functional photosynthetic electron transport (PET) chain, which may facilitate a rapid acclimation to more favorable light conditions in spring (Peters and Thomas 1996). In many of our treatments, growth rate, $F_v:F_m$, and σ_{PSII} were appreciably uncoupled.

When cells were grown under the combined low-iron and low-light growth condition (−FeLL), all isolates experienced significant decreases in growth rate of at least 35% (ANOVA, $p < 0.05$) relative to +FeSL cultures (Online Resource 2). However, significant declines in $F_v:F_m$ compared to the maximum $F_v:F_m$ in +FeSL cultures were only evident in *F. cylindrus* (Mann–Whitney, $p = 0.01$) and *Navicula* sp. Increases in $F_v:F_m$ in the −FeLL treatment were observed in *A. actinochilus*, and *E. antarctica*. An increase in σ_{PSII} of $\sim 30\%$ ($p < 0.05$) relative to the minimum σ_{PSII} in +FeSL was observed in *F. cylindrus*, *P. alata* (Mann–Whitney; $p = 0.024$), and *C. cf. sociales*. Steady-state measurements of growth in *T. antarctica* in −FeLL were not obtainable due to the cessation of cell growth.

The diatoms isolated for this study represent a wide range of cell sizes and biovolumes. Biovolumes per cell for the isolates ranged across five orders of magnitude from $50 \mu\text{m}^3$ for *F. cylindrus* to $> 10^5 \mu\text{m}^3$ for *T. antarctica* (Online Resource 2). To examine how cell size may affect growth under low-iron and/or low-light conditions, we compared diatom biovolume to the μ_{max} as well as $\mu:\mu_{\text{max}}$ under low-iron (Fe effect) and low-light (light effect) conditions. In replete conditions, μ_{max} was not significantly correlated with biovolume ($r = -0.51$, $p = 0.16$; Online Resource 2). Similarly, under low-iron or low-light conditions, there was not a significant correlation between $\mu:\mu_{\text{max}}$ and biovolume (Fe; $r = -0.36$, $p = 0.35$ and light; $r = -0.28$, $p = 0.47$; Online Resource 2).

Transcriptome sequence library sizes ranged from 678,857 (*Navicula* sp.) to 2,127,016 (*E. antarctica*) paired-end reads (Table 2). Assemblies yielded transcriptomes with

7017 contigs (*E. antarctica*, N50 = 327) to 30,791 contigs (*P. subcurvata*, N50 = 1265). The minimum length of a contig was 200 base pairs (bp) in all transcriptomes and the average contig length was between 330 bp (*E. antarctica*) to 881 bp (*P. subcurvata*; Table 2). Mapping reads back to the assembled transcriptome resulted in mapping efficiencies of 12% (*E. antarctica*) to 54% (*T. antarctica*). Functional annotation was provided with KAAS tBLASTn comparison against the KEGG database. The single-directional best-hit method was used, yielding transcriptomes with 12–24% functionally annotated contigs (Table 2).

In addition to reporting N50 values, each de novo assembly was assessed for contiguity and completeness. Contiguity analysis yielded transcriptomes with 0.07 (*C. cf. sociales*) to 0.25 (*P. subcurvata*) coverage values, indicating there are many partial genes within our transcriptomes. Ideally, the distribution of contigs that cover a reference gene should be closer to 1. However, in the case of *Navicula* sp., a mid-range quality transcriptome, contiguity was 0.16 (Online Resource 2).

Quality metrics of transcriptome completeness were calculated with BUSCO and KEGG mapping tools. Using the eukaryote BUSCO gene set allowed for assessing the presence of 303 highly conserved genes within our transcriptomes. Through assessing both the complete and fragmented orthologs, coverage of our transcriptomes ranged from 16% (*E. antarctica*) to 74% (*P. subcurvata*) (Table 2). As a comparison, the BUSCO scores of strains of *E. antarctica*, *T. antarctica*, and *P. alata* sequenced as part of the MMETSP were between 66 and 80%. Despite the slightly lower scores of our transcriptomes for *T. antarctica* and *P. alata* (71 and 42%, respectively), there is excellent agreement with gene presence/absence between these diatoms and those of the same species sequenced as part of MMETSP (Fig. 3). Indeed, the *E. antarctica* strain in our study had the lowest sequencing depth and gene coverage, although we were able to recover additional genes of interest by querying a strain sequenced as part of the MMETSP (Fig. 3). Nonetheless, the absence of key genes of interest queried in this study for isolates with low transcriptome completeness (i.e., *C. cf. sociales*) should be interpreted with caution.

We investigated 20 protein-encoding genes potentially involved in iron and/or light stress responses in our isolates, and the isolates sequenced as part of the MMETSP. Protein substitution is a common strategy used by diatoms in photosynthesis to reduce their Fe requirements. When iron is scarce, diatoms will substitute iron-containing cytochrome c_6 (CYTC6) for copper-containing plastocyanin (PCYN) (Peers and Price 2006). *CYTC6* transcripts were detected in all our isolates, as well as in 95% of diatoms in the world's oceans, with no statistically significant difference in its biogeographical distribution (*Fisher's exact test*, $p = 0.999$) (Fig. 4, Online Resource 1).

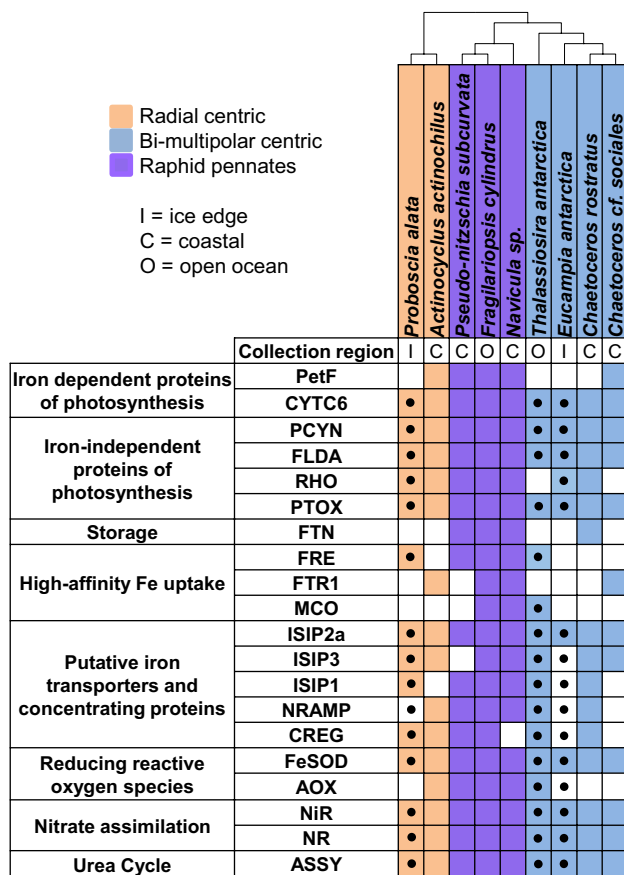


Fig. 3 A matrix depicting the presence of select iron-related genes in eight diatom transcriptomes and the genome of *F. cylindrus* color coded by their lineage: radial centric (orange), bi-multipolar centric (purple), and raphid pennate (blue). An 18S rDNA phylogenetic tree has been placed above the gene matrix for reference. Isolation source indicates the environment in which the diatoms were isolated: *O* open ocean, *I* sea ice edge, *C* coastal. Black circles indicate genes that are present in MMETSP transcriptomes of the same species (where available)

PCYN displayed a statistically significant biogeographical distribution with 95% of SO diatoms expressing *PCYN*, while only 22% of non-SO diatoms expressed the gene (most grown under replete conditions) (*Fisher's exact test*, $p < 0.001$). Transcripts for the redox substitution pair *CYTC6* and *PCYN* were found in all eight of our diatom transcriptomes (as well as the *F. cylindrus* genome; Mock et al. 2017).

Under low-iron conditions, diatoms will substitute flavodoxin (*FLDA*) for ferredoxin (*PetF*) in PET (La Roche et al. 1996). *PetF* transcripts were identified in *C. cf. sociales*, *Navicula sp.*, *A. actinochilus*, *P. subcurvata*, and *F. cylindrus*; however, *FLDA* was present in all of our isolates as well as 100% of SO diatom sequenced in the MMETSP (*Fisher's exact test*, $p < 0.001$). There was not a statistically significant biogeographical trend in the distribution of

PetF, although it was identified in only 32% of SO isolates (*Fisher's exact test*, $p = 0.144$) (Fig. 4, Online Resource 1).

Additional genes we investigated associated with photosynthetic ATP production that could be helpful to SO diatoms include plastid terminal oxidase (*PTOX*), proteorhodopsin (*RHO*), and mitochondrial alternative oxidase (*AOX*). First, in addition to linear electron transport, diatoms can synthesize ATP by creating an alternate cyclic electron pathway from photosystem II (*PSII*) to *PTOX*. There is no biogeographical trend in regard to the number of diatoms that possess *PTOX*, (*Fisher's exact test*, $p = 0.167$), and all the diatoms isolated in this study contained the gene. Second, *RHO* is a light-dependent proton pump that could compensate for a decreased production of ATP in Fe-limited cells (Raven 2013). While seven out of nine of the diatoms in this study contain *RHO* transcripts, it has previously been shown that this gene has a biogeographical distribution with more diatoms containing *RHO* in the Southern Ocean than in non-Southern Ocean regions (Marchetti et al. 2015). Finally, *AOX* is a mitochondrial membrane-bound, di-iron carboxylate protein which may participate in the reduction of oxygen species in cells at high-light irradiances (Bailleul et al. 2015). *AOX* is present in half of our isolates, although more diatoms from non-Southern Ocean regions (85%) were found to contain the gene compared to SO diatoms (*Fisher's exact test*, $p = 0.002$).

The high-affinity iron uptake system, which includes an iron permease (*FTR1*), a ferric reductase (*FER*), and a multi-copper oxidase (*MCO*), has a scattered presence in the isolates examined in this study. Only *F. cylindrus* (genome) and *Navicula sp.* have detectable transcripts from all three genes. *FRE* is commonly expressed in diatoms from non-Southern Ocean regions (89%), but is expressed in only half of SO diatoms (55%) (*Fisher's exact test*, $p = 0.001$). Additionally, most diatoms express an iron permease homolog in non-Southern Ocean regions (77%), whereas only 36% of diatoms from the Southern Ocean express *FTR1* ($p = 0.001$). 54% of non-SO diatoms appear to express a multi-copper oxidase, whereas only 36% of diatoms express the gene from the Southern Ocean ($p = 0.08$), although this may be a result of sequence divergence within *MCO* homologs (Groussman et al. 2015).

Low-iron responsive genes that may be putative iron transporters or that concentrate iron at the cell surface include *ISIP2a*, *ISIP1*, *ISIP3*, natural resistance-associated macrophage protein (*NRAMP*), and cellular repressor of E1A-genes (*CREG*) (Allen et al. 2008; Lommer et al. 2012; Morrissey et al. 2015). All SO diatoms possessed *ISIP2a*, whereas 88% of diatoms from non-Southern Ocean regions had detectable *ISIP2a* transcripts (*Fisher's exact test*, $p = 0.104$). Transcripts for *NRAMP* and *CREG* were more commonly found in the Southern Ocean than in the non-Southern Ocean regions (*Fisher's exact*

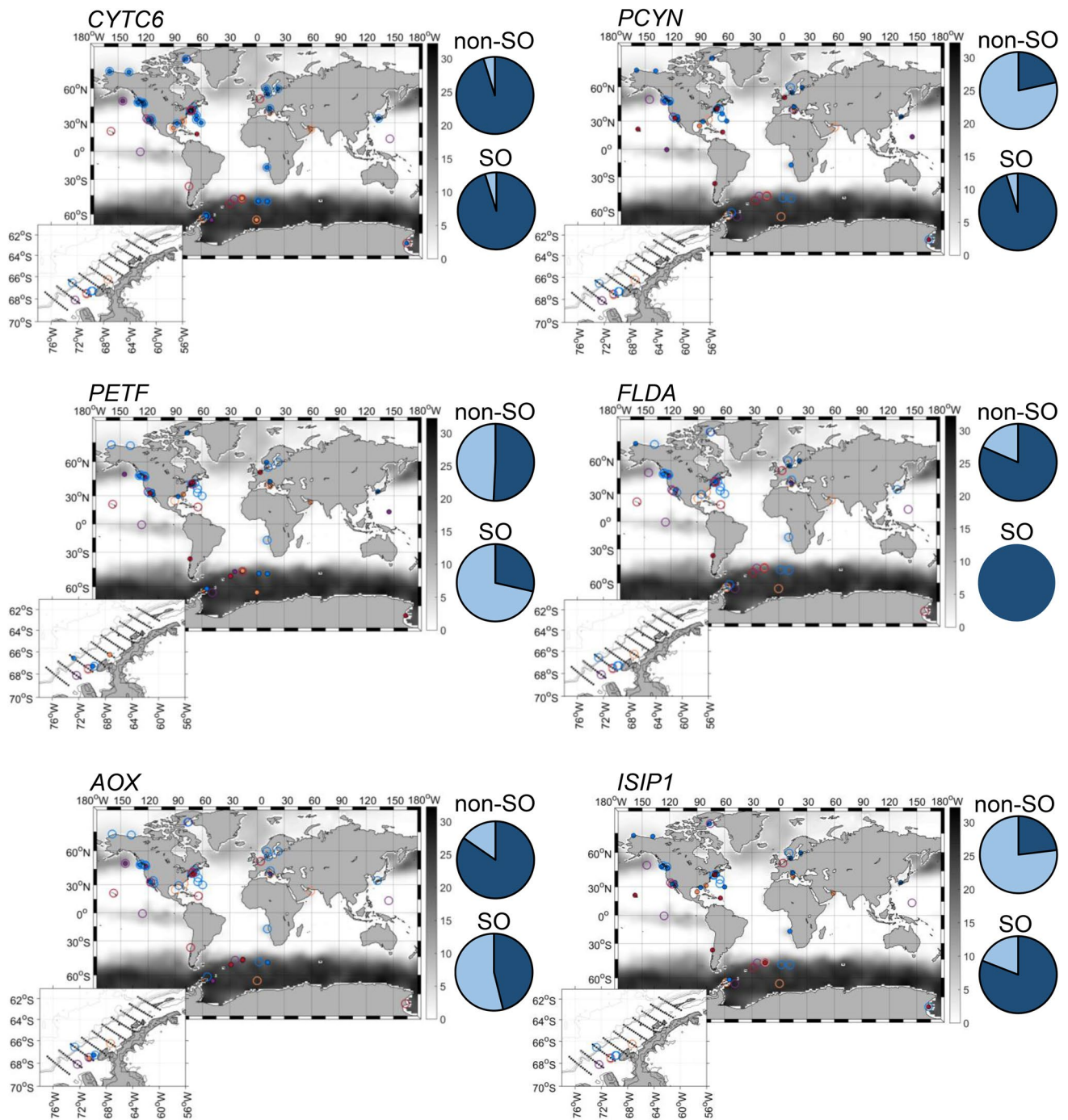


Fig. 4 Biogeography analysis of the presence of select iron-related genes in marine diatoms. The locations where strains have been isolated in which a gene is present (large open circles) or absent (small closed circles) within their transcriptomes or whole-genome sequences. Isolates are grouped according to diatom lineage (see Fig. 1 caption for color scheme). Background shading represents climatic

annual surface nitrate concentration ($\mu\text{mol l}^{-1}$) where high surface nitrate concentrations often reflect iron limitation. Nutrient data are from the World Ocean Atlas (Garcia et al. 2009). Inset figure displays a close-up of the WAP region. Pie charts represent the presence (dark blue) or putative absence (light blue) of a gene in SO diatoms compared to non-SO diatoms

test, $p = 0.017$ and 0.001 , respectively). Transcripts for *ISIP3* were detected in most diatoms regardless of isolation location (Fisher's exact test, $p = 0.018$) and 77%

of SO diatoms expressed *ISIP1*, whereas only 23% of non-SO diatoms expressed this gene (Fisher's exact test, $p < 0.001$).

Iron storage proteins such as ferritins (FTN) are needed for both short-term and long-term intracellular iron reserves (Marchetti et al. 2009). Only four diatoms in our study contained a detectable FTN; *Navicula* sp., *P. subcurvata*, *F. cylindrus*, and *C. rostratus*. FTN transcripts were detected in about half of the non-SO diatoms (54%), and thus there is not a greater prevalence of FTN among SO diatoms (*Fisher's exact test*, $p = 0.80$).

Finally, we queried the Fe metalloproteins involved in nitrogen metabolism and antioxidant stress. These included the iron-containing proteins nitrate (NR) and nitrite reductase (NiR) needed for nitrate assimilation, Fe-superoxide dismutase (*Fe-SOD*) which converts superoxide radicals to molecular oxygen and hydrogen peroxide (Peers and Price 2006), and the non-iron-containing enzyme arginosuccinate synthase (ASSY). Transcripts of NR, NiR, ASSY, and Fe-SOD were detected in all of our transcriptomes (as well as the *F. cylindrus* genome) and within diatoms with publically available genomes or transcriptomes, suggesting these genes are present in all diatoms.

Discussion

Physiological effects of low iron and low light on SO diatoms

Four environmental stress responses were observed: no interaction between iron and light, also termed an antagonistic effect, a response in which either light or iron was the main limiting factor or an additive interaction between iron and light (Fig. 2). Antagonism is observed when the combined effects of two factors are not larger, or smaller, than the sum of the individual effects. In this example, reducing both iron and light produces the same reduction in growth rate as if either iron or light were limiting. *C. cf. sociales*, *P. subcurvata*, *A. actinochilus*, and *Navicula* sp. growth can be classified as having an antagonistic effect between iron and light, as $-FeLL$ cultures were not significantly different from either $-FeSL$ or $+FeLL$. This would indicate an additive relationship between iron and light does not exist in these polar diatoms. In contrast, Sunda and Huntsman (1995) found that in temperate diatoms, iron-limited, low-light cells had reduced growth rates compared to iron-limited, high-light cells due to increased iron demands under low light in order to efficiently use PET. Similarly, we observed an additive effect in three of the nine examined diatoms—*F. cylindrus*, *T. antarctica* (no growth), and *P. alata*. In these diatoms, growth rates were reduced most in the combined low-iron and low-light treatment compared to either variable alone, suggesting they exhibit a similar physiological response to these environmental conditions. *T. antarctica*

and *F. cylindrus* are the largest and the smallest cells, respectively, indicating their comparable growth and photophysiological responses may be underpinned by similar mechanisms despite their appreciable difference in size.

E. antarctica demonstrated primarily light limitation with no additive effect on growth rate of low iron in the low-light cultures. A previous study induced iron limitation in *E. antarctica* through addition of DFB buffer (Strzepek et al. 2011), indicating that our low-iron treatment may not have been low enough to limit the growth of *E. antarctica*. In *C. rostratus*, the patterns in growth are mainly driven by irradiance as well. Under growth-saturating light conditions, low-iron availability resulted in a slightly reduced growth rate (12%; $p < 0.001$); however, a decrease in irradiance resulted in a much larger decrease in growth rate (45%; $p < 0.001$), and there was no further reduction in growth rate in the $-FeLL$ culture.

In the $-FeSL$ treatment, we observed a negative correlation between $F_v:F_m$ and in σ_{PSII} (a reduction in $F_v:F_m$ and an increase in σ_{PSII}) in more species than in the $+FeLL$ treatment. While growth rate was reduced in both treatments for all species (except for *F. cylindrus* in $-FeSL$, and *P. alata* in $+FeLL$) relative to the control, it was only in the $+FeLL$ treatment that $F_v:F_m$ and σ_{PSII} remain unchanged relative to $+FeSL$. These results suggest that at the light and iron levels used in this study, the photophysiology of diatoms was more sensitive to iron than light. This is perhaps due to the fact that SO diatoms have to cope with long periods of time in almost complete darkness and thus it would be advantageous if they retained functional PET which could facilitate a rapid acclimation to more favorable light conditions in spring (Peters and Thomas 1996). SO diatoms might have unique biophysical or molecular mechanisms to maintain an efficient photochemical yield and cross-sectional absorption area of PSII, despite a reduction in growth, as proposed by Strzepek et al. (2012). In temperate phytoplankton communities, light limitation, as well as iron, has been shown to influence $F_v:F_m$ and σ_{PSII} (Suggett et al. 2009), but SO diatoms exhibit smaller effects on light-limited growth and photophysiology compared to Fe (Strzepek et al. 2012). The diatoms in our study seemed to have no or minimal effects on $F_v:F_m$ and σ_{PSII} under light limitation compared to $-FeSL$ and the $-FeLL$ treatments. In the Southern Ocean, $F_v:F_m$ seems to be a good indicator of Fe limitation in some species and in natural phytoplankton populations (van Oijen et al. 2004; Alderkamp et al. 2012); however, among the diatoms with decreased growth in the low-Fe treatment used in this study, only three species showed a decreased $F_v:F_m$, while five species had increased σ_{PSII} , indicating that the negative correlation between these two measurements may not serve as a good indicator of Fe limitation in all SO diatoms.

The lack of an additive effect for most of the examined diatoms supports the findings of Strzepek et al. (2012), in

which iron and light limitation in SO diatoms could result in a photoacclimatory response that largely increases the size but not the number of photosynthetic units (PSUs) under low-light conditions, thereby minimizing increases in iron demands associated with increasing numbers of PSUs. The greater effect of decreased light on growth rate, and the fact that most Fe-limited diatoms were not subject to further reductions in growth rate at low light, indicate the majority of SO diatoms are less likely to experience an additive effect of low iron and low light than are diatoms from temperate regions. However, in scenarios where light-limited diatoms experience a higher degree of Fe limitation, then it may be possible they experience an additive co-limitation.

Phytoplankton cell size is known to correlate with resource utilization and growth (Eppley et al. 1969); however, it appears that the ability of SO diatoms to grow at low iron and light levels does not scale with biovolume. Diatoms in this study displayed an insignificant correlation between biovolume and maximum growth rates and relative growth rates under low-iron and low-light conditions. A lack of correlation between maximum growth rates and biovolume was also observed among other SO diatoms (Strzepek et al. 2011). Iron uptake rates per unit of cell volume of marine algal species are inversely related to mean cell diameter due to decreases in cell surface-to-volume ratios (SA:V) (Sunda and Huntsman 1995; Lis et al. 2015). Thus, small cells should dominate HNLC regions; however, iron uptake and growth kinetics are not the only factors that influence cell size. Having a large biovolume offers possible protection from zooplankton grazing, provides high-nutrient storage capabilities via large vacuoles (Eppley et al. 1969), and allows diatoms to regulate their buoyancy and chemical composition to stay in the photic zone (Richardson and Cullen 1995). Taken together, these characteristics suggests large, SO diatoms may have acquired biochemical mechanisms that enable them to maintain relatively high growth rates under stressful conditions. The genes we found to be biogeographically more prevalent in the Southern Ocean—FLDA, RHO, PCYN, and ISIP1—are an indication that SO diatoms have the molecular potential that allow them to grow at high maximum and relative growth rates under low-iron conditions despite their large size.

Molecular bases for iron and light limitation responses in SO diatoms

Phenotypic variability in growth rates and photophysiology as a function of iron and/or light status observed among the diatoms examined in this study could likely be explained by differences in gene repertoires in relation to iron-requiring processes such as iron acquisition and homeostasis, photosynthesis, and nitrogen assimilation. These genes fall

into eight functional categories, including photosynthetic iron-dependent and iron-independent proteins, internal iron storage proteins, high-affinity iron uptake proteins, putative transport and plasmalemma iron-concentrating proteins, superoxide dismutase and alternative oxidase proteins, nitrogen assimilation proteins, and proteins involved in the urea cycle (Fig. 3).

Selective pressure in low-iron environments has resulted in diatoms evolving strategies to meet their high-iron demands. One of the most conspicuous strategies is protein substitution within PET. All sequenced diatom genomes have *CYTC6*, but only certain diatoms, particularly those isolated from low-iron regions, such as *T. oceanica* and *F. cylindrus*, appear to have *PCYN* (Raven 2013). *CYTC6* and *PCYN* transcripts were found in all eight of our SO diatom transcriptomes, suggesting that while *PCYN* is likely beneficial for growth in HNLC environments, it does not preclude the expression of *CYTC6*. These two proteins are functionally very similar in their molecular mass as well as their ability to transfer electrons; thus, their expression in the Southern Ocean might largely be based on whether copper or iron is more readily available (Raven et al. 1999).

Although we did not focus extensively on gene expression in this study, we observed higher relative transcripts for *PCYN* than *CYTC6* in 5 of the 8 diatom transcriptomes. Because our culture conditions were iron replete, this suggests that these diatoms may prefer *PCYN* under all growth conditions. The oceanic centric diatom, *T. oceanica*, constitutively expresses *PCYN* even under iron-replete conditions, suggesting that *PCYN* expression is a permanent adaptation to low-iron, open-ocean environments (Peers and Price 2006). In the case of *T. antarctica*, transcripts for *CYTC6* were ~ 19-fold higher than those for *PCYN*, suggesting this species possibly relies primarily on *CYTC6* for electron transport under Fe-replete conditions (Online Resource 1). In our physiological study, *T. antarctica* had the lowest relative growth rate under low-iron conditions, suggesting this species is accustomed to growing under high-iron conditions. In the strain of *T. antarctica* sequenced as part of the MMETSP, transcripts were present for both of these genes. *CYTC6* is present throughout the MMETSP diatoms, illustrating that it is a ubiquitous component of PET although the extent to which it is expressed in each diatom is unknown. The presence of *PCYN* does have a strong biogeographical pattern with 95% of SO diatoms expressing transcripts for the gene, whereas only 22% of non-SO diatoms (grown under replete conditions) expressed the gene. Thus, SO diatoms may rely more on *PCYN* either under Fe-replete conditions or in response to low-iron availability.

Ferredoxin (PetF) contains two iron-sulfur clusters per electron transport molecule, while flavodoxin (FLDA) contains a flavin, rather than iron, as a redox center. Some iron-limited diatoms have been found to substitute FLDA

for PetF to transport electrons from PSI to NADP reductase in the enzymatic production of NADPH (Erdner et al. 1999). While *FLDA* was present in all transcriptomes (and the *F. cylindrus* genome), *PetF* transcripts were only identified in *C. cf. sociales*, *Navicula* sp., *A. actinochilus*, *P. subcurvata*, and *F. cylindrus*. Although not a measure of gene expression, the transcription of *PetF* was particularly high for *Navicula* sp., with ~ 20 times higher RPKM values of *PetF* than *FLDA*, suggesting that ferredoxin is preferentially utilized over flavodoxin under high-iron conditions in this species. By contrast, the other diatoms had low transcript abundance of *PetF* (< 100 transcripts) in the Fe-replete cultures. The possible lack of detection of *PetF* in *E. antarctica* could be due to the small size of the transcriptome. Relative transcript abundances of *FLDA* were particularly high in *P. alata* and *C. rostratus* (> 19,000 transcripts), perhaps reflecting constitutive expression of *FLDA* instead of *PetF*, or complete lack of dependence on *PetF* altogether. The high abundance of *FLDA* transcripts under Fe-replete conditions indicates this might be a permanent adaptation. These species may rely heavily on substitution strategies, and their high relative growth rates under low-Fe conditions (> 87% of μ_{\max}) could be attributed, in part, to their dependence on *FLDA* as well as other non-iron-containing protein substitutes. Other polar diatoms, such as *Fragilariopsis curta* and a *Pseudo-nitzschia* sp., appear to only express *FLDA* and do not transcribe *PetF* (Pankowski and Mcminn 2008). Biogeographically, *PetF* and *FLDA* distributions tend to depend on their location of isolation, with more diatoms containing *FLDA* and fewer diatoms containing *PetF* in the SO diatoms, suggesting a reduced dependence on iron-containing proteins like *PetF*.

Diatoms may also use a plastid terminal oxidase (PTOX) to create a proton gradient for ATP synthesis via a short, alternate pathway from photosystem II (PSII) to PTOX, in the reduction of photosynthetically produced molecular O₂ back to water. Under low-iron conditions, employing the PTOX electron shunt is advantageous, as it only requires two iron atoms to produce ATP (but not NADPH), whereas the cytochrome *b₆f* and photosystem I (PSI) complexes use 17 iron atoms (Behrenfeld and Milligan 2013). Upregulation of PTOX may also serve to protect PSII reaction centers by acting as a safety valve for excess PET electrons (Nawrocki et al. 2014). In our biogeographical analysis, most diatoms contained *PTOX*, regardless of their isolation location ($p = 0.167$). Furthermore, all diatoms in this study expressed *PTOX*, indicating this cyclic pathway may have an important role in protection or acclimation to low-iron or variable light conditions (Yoshida et al. 2007).

Rhodopsins (*RHO*) can be used as an iron/light management strategy as it provides a low-iron alternative to photosynthesis for the production of ATP (Marchetti et al. 2015). While not as energetically efficient as cyclic

electron flow within PSUs, *RHO* could compensate for a decrease in energy production in Fe-limited cells (Fuhrman et al. 2008). By querying the MMETSP database, Marchetti et al. (2015) demonstrated that diatoms from the Southern Ocean more often contained *RHO* when compared to those from non-Southern Ocean regions, suggesting the gene may have a particularly useful role in low-iron regions such as the Southern Ocean. Of our sequenced diatoms, seven out of nine isolates possessed the gene. *T. antarctica* and *C. cf. sociales* lacked detectable transcripts of *RHO*, perhaps contributing to the low relative growth rates of both species under low-iron conditions. We cannot conclude the absence of *RHO* in *T. antarctica*, although we did not detect the gene in the MMETSP transcriptome of another *T. antarctica* strain. The lack of a detectable *RHO* in *C. cf. sociales* may be due to sequencing depth. In contrast, *P. alata* had high relative transcript abundance for *RHO* and minimal reduction in growth rate under our low-iron conditions, suggesting that *P. alata* might lower its iron requirements by partial energy production through proteorhodopsin.

Physiological and molecular studies of *T. oceanica* have shown that one or more high-affinity iron uptake systems may be induced which exist under low-iron conditions (Lommer et al. 2012). In one such system, a ferric reductase (*FRE*) first reduces Fe(III) complexes to unchelated Fe(II), which is then re-oxidized by a multi-copper oxidase (*MCO*) that is paired with an iron permease (*FTR1*) which transports Fe(III) into the cell (Marchetti and Maldonado 2016). Seven out of nine species lacked transcripts for at least one component of the high-affinity iron uptake system or lacked the system altogether. *F. cylindrus* (genome) and *Navicula* sp. possessed the transcripts for all the genes. While *F. cylindrus* and *P. alata* seemed functionally similar, both displaying an additive interaction response between iron and light, their acquisition strategies appear to be fundamentally different, as *P. alata* appears to only express *FRE*. Transcripts for the entire high-affinity iron uptake system appear to be more common in diatoms from lower latitudes suggesting that SO diatoms may have alternative iron acquisition mechanisms.

An iron-starvation-induced iron-binding protein (*ISIP2a*) is widely expressed among eukaryotic phytoplankton and can concentrate Fe(III) at the cell surface without the use of *MCO* (Morrissey et al. 2015). There was no biogeographical pattern associated with the distribution of *ISIP2a* and was present in most diatoms; thus it seems to be a highly conserved and important protein (*Fisher's exact test*, $p = 0.104$). Similar to *ISIP2a*, transcripts for *ISIP3* were detected in most diatoms regardless of isolation location ($p = 0.018$). Interestingly, 77% of SO diatoms expressed *ISIP1*, whereas only 23% of non-SO diatoms expressed this gene (Fig. 4). In *T. oceanica*, *ISIP1* was found to have multiple paralogous versions and a protein structure that is predicted to be

a low-iron inducible ferric receptor (Lommer et al. 2012). While the function of ISIP1 in cellular iron uptake remains speculative, it is only found in diatoms and haptophytes and is one of the most highly expressed genes under iron limitation (Morrissey et al. 2015).

Another proposed low-Fe responsive gene is NRAMP, a protein predicted to be involved in vacuolar Fe storage that is upregulated under low-Fe conditions in some diatoms (Kustka et al. 2007; Morrissey and Bowler 2012). The gene was detected in all of our transcriptomes (except for *C. cf. sociales*, likely due to the low sequencing coverage of this isolate), and was more common in the Southern Ocean than at lower latitudes, suggesting that NRAMP could be useful in low-iron waters of the Southern Ocean. Transcripts for CREG were detected in all transcriptomes except for *Navicula* sp. and *C. cf. sociales*. CREG was more commonly found in the Southern Ocean than in non-Southern Ocean regions, again, suggesting it may play a role in helping diatoms cope with low-iron availability. The ISIPs, NRAMP, and CREG may be common in the Southern Ocean where iron is limiting, as they would increase the number of surface receptors and transporters, overall increasing the affinity for iron at the cell surface (Lommer et al. 2012).

At high intracellular concentrations, iron can be toxic, and as the rate of supply and metabolic demand can be quite variable, ferritins (FTN) can be used for both short-term and long-term intracellular iron storage. Iron storage may vary in response to iron supply, cellular metabolism, and growth demand linked to the diel light–dark cycle (Marchetti et al. 2009; Botebol et al. 2015). Almost all raphid pennate diatoms for which whole-genome sequences or transcriptomes are available contain at least one ferritin gene, whereas FTN in centric diatoms appear to be more randomly distributed (Groussman et al. 2015). Only four diatoms in our study contained a detectable FTN; the raphid pennate diatoms *Navicula* sp., *P. subcurvata*, and *F. cylindrus* (genome), as well as the bi-multipolar centric diatom *C. rostratus*. Ferritin has been identified in all four clades of diatoms, with paralogs present in many species, possibly being introduced by lateral gene transfer (Marchetti et al. 2009; Groussman et al. 2015). Similar to SO diatoms, FTN transcripts were detected in about half of the non-SO diatoms (54%) and thus there does not appear to be a greater prevalence of FTN among SO diatoms.

Diatoms utilize a number of antioxidant enzymes to minimize reactive oxygen species produced as byproducts of photosynthesis and other metabolic processes. Many algae have both Fe-SOD and Mn-SOD, but may preferentially express Mn-SOD under iron-limiting conditions to reduce iron demands (Maldonado et al. 2006; Groussman et al. 2015). In our analysis, all of our isolates expressed transcripts of Fe-SOD, and in fact all diatoms within the MMETSP possessed this gene, verifying that it is an important component

to minimizing reactive oxygen species. Another oxidative stress enzyme, mitochondrial alternative oxidases (AOX), reduces ROS in mitochondria (Baxter et al. 2007). Excess electrons from photosynthesis can also be transported via the malate shunt to the mitochondria, where AOX will utilize them to reduce molecular O₂ to H₂O, producing ATP in the process (Yoshida et al. 2007). The presence of AOX transcripts appears to be more common in non-SO diatoms, where 85% contain a gene homolog compared to only 50% of SO diatoms (Fig. 4). In *P. tricorutum*, AOX inhibition was associated with decreased photosynthetic activity under high-light conditions (Bailleul et al. 2015). Thus, AOX may be more prominent in non-Southern Ocean regions where higher average light intensities are common, and could be advantageous for optimizing photosynthesis in these environments.

Conclusion

Our transcriptomes suggest a variety of gene repertoires in polar diatoms that may contribute to the generally lower iron and light requirements of SO diatoms (Strzepek et al. 2011, 2012). *P. subcurvata*, *F. cylindrus*, and *C. cf. sociales* were grouped based on having relatively higher μ_{\max} and smaller size. Despite the lower quality transcriptome in *C. cf. sociales*, these species appear to have similar gene repertoires. Given the larger sizes of *T. antarctica*, *P. alata*, *A. actinochilus*, and *E. antarctica*, it is surprising these diatoms appear to lack ferritin and a complete high-affinity uptake system as gathered from our transcriptomes and those from the MMETSP. *T. antarctica* and *A. actinochilus* have some components of this uptake system; however, they exhibited the largest reductions in growth rates under low-iron/light conditions, and thus might not be as competitive in these environments when compared to some of the other examined diatoms.

Although additional diatom transcriptomes would provide for a more complete understanding of whether there are biogeographical patterns associated with these genes, some initial insights have been gained from our analysis. One outcome of our combined physiological and transcriptomic study is that genes can be targeted for molecular indicators of iron and light limitation within SO diatom assemblages. Previous research has used the expression ratio of proteins and genes sensitive to iron levels as molecular indicators of iron nutritional status; these include flavodoxin-to-ferredoxin ratios (La Roche et al. 1996); FLDA and ISIP3 in *T. oceanica* (Chappell et al. 2014); and ISIP2a to FTN ratios in *P. granii* (Marchetti et al. 2017). Although our study does not provide an analysis of gene expression, our data suggest that differential gene expression approaches may be useful in identifying molecular indicators of iron

and light physiological status of diatoms from the Southern Ocean. From our study, ferredoxin, flavodoxin, ferritin, rhodopsin, plastocyanin, alternative mitochondrial oxidase, cytochrome c_6 , and the ISIP genes appear to be present in most (but not all) diatom clades and are thus good candidates for reflecting their iron status and long-term adaptation to low-iron conditions. Ultimately, by studying gene repertoires in combination with assessing physiological attributes, we can begin to uncover additional cellular mechanisms that influence diatom distribution and abundance.

Acknowledgements This study was funded by the National Science Foundation Grant PLR1341479 awarded to AM, and NSF Grant OPP1043339 to NC. MMETSP was funded in part by the Gordon and Betty Moore Foundation through Grant 2637 to the National Center for Genome Resources. CMM was primarily supported by a Gates Millennium Fellowship. We thank S. Nelson and J. Benjamin for assistance with diatom culturing, M. Kanke and J. Kim for scripting assistance, and B. MacGregor and W. Sunda for helpful comments on the manuscript.

References

- Agusti S, Duarte CM (2000) Experimental induction of a large phytoplankton bloom in Antarctic coastal waters. *Mar Ecol Prog Ser* 206:73–85. <https://doi.org/10.3354/meps206073>
- Alderkamp AC, Kulk G, Buma AGJ et al (2012) The effect of iron limitation on the photophysiology of *Phaeocystis antarctica* (prymnesiophyceae) and *Fragilariopsis cylindrus* (bacillariophyceae) under dynamic irradiance. *J Phycol* 48:45–59. <https://doi.org/10.1111/j.1529-8817.2011.01098.x>
- Allen AE, Laroche J, Maheswari U et al (2008) Whole-cell response of the pennate diatom *Phaeodactylum tricorutum* to iron starvation. *Proc Natl Acad Sci* 105:10438–10443. <https://doi.org/10.1073/pnas.0711370105>
- Altschul SF, Gish W, Miller W et al (1990) Basic local alignment search tool. *J Mol Biol* 215:403–410. [https://doi.org/10.1016/S0022-2836\(05\)80360-2](https://doi.org/10.1016/S0022-2836(05)80360-2)
- Arrigo KR, van Dijken GL, Bushinsky S (2008) Primary production in the Southern Ocean, 1997–2006. *J Geophys Res* 113:C08004. <https://doi.org/10.1029/2007JC004551>
- Arrigo KR, Mills MM, Kropuenske LR et al (2010) Photophysiology in two major southern ocean phytoplankton taxa: photosynthesis and growth of *Phaeocystis antarctica* and *Fragilariopsis cylindrus* under different irradiance levels. *Integr Comp Biol* 50:950–966. <https://doi.org/10.1093/icb/icq021>
- Bailleul B, Berne N, Murik O et al (2015) Energetic coupling between plastids and mitochondria drives CO₂ assimilation in diatoms. *Nature* 524:366–369. <https://doi.org/10.1038/nature14599>
- Baxter CJ, Redestig H, Schauer N et al (2007) The metabolic response of heterotrophic *Arabidopsis* cells to oxidative stress. *Plant Physiol* 143:312–325. <https://doi.org/10.1104/pp.106.090431>
- Behrenfeld MJ, Milligan AJ (2013) Photophysiological expressions of iron stress in phytoplankton. *Ann Rev Mar Sci* 5:217–246. <https://doi.org/10.1146/annurev-marine-121211-172356>
- Blain S, Quéguiner B, Armand L et al (2007) Effect of natural iron fertilization on carbon sequestration in the Southern Ocean. *Nature* 446:1070–1074. <https://doi.org/10.1038/nature05700>
- Botebol H, Lesuisse E, Sutak R et al (2015) Central role for ferritin in the day/night regulation of iron homeostasis in marine phytoplankton. *Proc Natl Acad Sci* 112:1–6. <https://doi.org/10.1073/pnas.1506074112>
- Bowler C, Allen AE, Badger JH et al (2008) The *Phaeodactylum* genome reveals the evolutionary history of diatom genomes. *Nature Lett* 456:239–244
- Boyd PW (2002) Environmental factors controlling phytoplankton processes in the Southern Ocean. *J Phycol* 38:844–861
- Boyd PW, Watson AJ, Law CS et al (2000) A mesoscale phytoplankton bloom in the polar Southern Ocean stimulated by iron fertilization. *Nature* 407:695–702. <https://doi.org/10.1038/35037500>
- Boyd PW, Crossley AC, DiTullio GR et al (2001) Control of phytoplankton growth by iron supply and irradiance in the subantarctic Southern Ocean: experimental results from the SAZ Project. *J Geophys Res* 106:31573. <https://doi.org/10.1029/2000JC000348>
- Boyd PW, Jickells T, Law CS et al (2007) Mesoscale iron enrichment experiments 1993–2005: synthesis and future directions. *Science* 315:612–617. <https://doi.org/10.1126/science.1131669>
- Brand LE, Guillard RL, Murphy LS (1981) A method for the rapid and precise determination of acclimated phytoplankton reproduction rates. *J Plankton Res* 3:193–201
- Cassar N, Bender ML, Barnett BA et al (2007) The Southern Ocean biological response to aeolian iron deposition. *Science* 317:1067–1070. <https://doi.org/10.1126/science.1144602>
- Edgar RC (2004) MUSCLE: multiple sequence alignment with high accuracy and high throughput. *Nucleic Acids Res* 32:1792–1797. <https://doi.org/10.1093/nar/gkh340>
- Edwards R, Sedwick P, Land E (2001) Iron in East Antarctic snow-implications for atmospheric iron deposition and algal production in Antarctic waters. *Geophys Res Lett* 28:3907–3910. <https://doi.org/10.1029/2001GL012867>
- Eppley RW, Rogers JN, McCarthy JJ (1969) Half-saturation constants for uptake of nitrate and ammonium by marine phytoplankton. *Limnol Oceanogr* 14:912–920
- Erdner DL, Price NM, Doucette GJ et al (1999) Characterization of ferredoxin and flavodoxin as markers of iron limitation in marine phytoplankton. *Mar Ecol Prog Ser* 184:43–53
- Feng Y, Hare CE, Rose JM et al (2010) Interactive effects of iron, irradiance and CO₂ on Ross Sea phytoplankton. *Deep Res Part I Oceanogr Res Pap* 57:368–383. <https://doi.org/10.1016/j.dsr.2009.10.013>
- Fuhrman JA, Schwalbach MS, Stingl U (2008) Proteorhodopsins: an array of physiological roles? *Nat Rev Microbiol* 6:488–494
- Gorbunov MY, Falkowski PG (2005) Fluorescence induction and relaxation (FIRE) technique and instrumentation for monitoring photosynthetic processes and primary production. In: Van der Est A, Bruce D (eds) *Photosynthesis: fundamental aspects to global perspectives: proceedings of the 13th international congress on photosynthesis*, Allen and Unwin, London, pp 1029–1031
- Grabherr MG, Haas BJ, Yassour M et al (2011) Full-length transcriptome assembly from RNA-Seq data without a reference genome. *Nat Biotechnol* 29:644–652. <https://doi.org/10.1038/nbt.1883>
- Greene RM, York N, Geider RJ, Falkowski PG (1991) Effect of iron limitation on photosynthesis in a marine diatom. *Limnol Oceanogr* 36:1772–1782
- Groussman RD, Parker MS, Armbrust EV (2015) Diversity and evolutionary history of iron metabolism genes in diatoms. *PLoS ONE* 10:e0129081. <https://doi.org/10.1371/journal.pone.0129081>
- Hillebrand H, Dürselen CD, Kirschtel D et al (1999) Biovolume calculation for pelagic and benthic microalgae. *J Phycol* 35:403–424. <https://doi.org/10.1046/j.1529-8817.1999.3520403.x>
- Hoppe CJM, Holtz LM, Trimbom S, Rost B (2015) Ocean acidification decreases the light-use efficiency in an Antarctic diatom under dynamic but not constant light. *New Phytol* 207:159–171. <https://doi.org/10.1111/nph.13334>

- Hubbard KA, Rocap G, Armbrust EV (2008) Inter- and intraspecific community structure within the diatom genus *Pseudo-nitzschia* (Bacillariophyceae). *J Phycol* 44:637–649. <https://doi.org/10.1111/j.1529-8817.2008.00518.x>
- Jukes TH, Cantor CR (1969) Evolution of protein molecules. In: Munro HN (ed) *Mammalian Protein Metabolism*. Academic Press, New York, pp 21–132.
- Kanehisa M, Goto S, Hattori M et al (2006) From genomics to chemical genomics: new developments in KEGG. *Nucleic Acids Res* 34:D354–D357. <https://doi.org/10.1093/nar/gkj102>
- Kearse M, Moir R, Wilson A et al (2012) Geneious basic: an integrated and extendable desktop software platform for the organization and analysis of sequence data. *Bioinformatics* 28:1647–1649. <https://doi.org/10.1093/bioinformatics/bts199>
- Keeling PJ, Burki F, Wilcox HM et al (2014) The marine microbial eukaryote transcriptome sequencing project (MMETSP): illuminating the functional diversity of eukaryotic life in the oceans through transcriptome sequencing. *PLoS Biol* 12:e1001889. <https://doi.org/10.1371/journal.pbio.1001889>
- Kropuenske LR, Mills MM, van Dijken GL et al (2009) Photophysiology in two major Southern Ocean phytoplankton taxa: photoprotection in *Phaeocystis antarctica* and *Fragilariopsis cylindrus*. *Limnol Oceanogr* 54:1176–1196. <https://doi.org/10.4319/lo.2009.54.4.1176>
- Kustka AB, Allen AE, Morel FMM (2007) Sequence analysis and transcriptional regulation of iron acquisition genes in two marine diatoms. *J. Phycol.* 43:715–729. <https://doi.org/10.1111/j.1529-8817.2007.00359.x>
- La Roche J, Boyd PW, McKay RML, Geider RJ (1996) Flavodoxin as an in situ marker for iron stress in phytoplankton. *Nature* 382:802–805
- Langmead B, Salzberg SL (2012) Fast gapped-read alignment with Bowtie 2. *Nat Methods* 9:357–359. <https://doi.org/10.1038/nmeth.1923>
- Li B, Ruotti V, Stewart RM et al (2009) RNA-Seq gene expression estimation with read mapping uncertainty. *Bioinformatics* 26:493–500. <https://doi.org/10.1093/bioinformatics/btp692>
- Lis H, Shaked Y, Kranzler C et al (2015) Iron bioavailability to phytoplankton: an empirical approach. *ISME J* 9:1003–1013. <https://doi.org/10.1038/ismej.2014.199>
- Lommer M, Specht M, Roy AS et al (2012) Genome and low-iron response of an oceanic diatom adapted to chronic iron limitation. *Genome Biol* 13:R66. <https://doi.org/10.1186/gb-2012-13-7-r66>
- MacIntyre HL, Cullen JJ (2005) Using cultures to investigate the physiological ecology of microalgae. In: Andersen RA (ed) *Algal Culturing Techniques*. Academic Press, New York, pp 287–326
- Maldonado MT, Allen AE, Chong JS et al (2006) Copper-dependent iron transport in coastal and oceanic diatoms. *Limnol Oceanogr* 51:1729–1743. <https://doi.org/10.4319/lo.2006.51.4.1729>
- Marchetti A, Harrison PJ (2007) Coupled changes in the cell morphology and the elemental (C, N, and Si) composition of the pennate diatom *Pseudo-nitzschia* due to iron deficiency. *Limnol Oceanogr* 52:2270–2284
- Marchetti A, Maldonado MT (2016) Iron. In: Borowitzka MA et al (eds) *Developments in applied phycology*. Springer, Switzerland, pp 233–279
- Marchetti A, Parker MS, Moccia LP et al (2009) Ferritin is used for iron storage in bloom-forming marine pennate diatoms. *Nature* 457:467–470. <https://doi.org/10.1038/nature07539>
- Marchetti A, Schrueth DM, Durkin CA et al (2012) Comparative metatranscriptomics identifies molecular bases for the physiological responses of phytoplankton to varying iron availability. *Proc Natl Acad Sci USA* 109:E317–E325. <https://doi.org/10.1073/pnas.1118408109>
- Marchetti A, Catlett D, Hopkinson BM et al (2015) Marine diatom proteorhodopsins and their potential role in coping with low iron availability. *ISME J* 9:1–4. <https://doi.org/10.1038/ismej.2015.74>
- Martin JH (1990) Glacial-interglacial CO₂ change: the iron hypothesis. *Paleoceanography* 5:1–13. <https://doi.org/10.1029/pa005i001p00001>
- Martin JA, Wang Z (2011) Next-generation transcriptome assembly. *Nat Rev Genet* 12:671–682. <https://doi.org/10.1038/nrg3068>
- Medlin L, Elwood HJ, Stickel S, Sogin ML (1988) The characterization of enzymatically amplified eukaryotic 16S-like rRNA-coding regions. *Gene* 71:491–499. [https://doi.org/10.1016/0378-1119\(88\)90066-2](https://doi.org/10.1016/0378-1119(88)90066-2)
- Mock T, Otilar RP, Strauss J et al (2017) Evolutionary genomics of the cold-adapted diatom *Fragilariopsis cylindrus*. *Nature Lett* 541:536–540. <https://doi.org/10.1038/nature20803>
- Montes-Hugo M, Martinson D, Ducklow HW et al (2009) Recent changes in phytoplankton communities associated with rapid regional climate change along Western Antarctic Peninsula. *Science* 323:1470–1473. <https://doi.org/10.1126/science.1164533>
- Moore JK, Abbott MR (2000) Phytoplankton chlorophyll distributions and primary production in the Southern Ocean. *J Geophys Res* 105:28709. <https://doi.org/10.1029/1999JC000043>
- Moriya Y, Itoh M, Okuda S et al (2007) KAAS: an automatic genome annotation and pathway reconstruction server. *Nucleic Acids Res* 35:182–185. <https://doi.org/10.1093/nar/gkm321>
- Morrissey J, Bowler C (2012) Iron utilization in marine cyanobacteria and eukaryotic algae. *Front Microbiol* 3:1–13. <https://doi.org/10.3389/fmicb.2012.00043>
- Morrissey J, Sutak R, Paz-Yepes J et al (2015) A novel protein, ubiquitous in marine phytoplankton, concentrates iron at the cell surface and facilitates uptake. *Curr Biol* 25:364–371. <https://doi.org/10.1016/j.cub.2014.12.004>
- Mortazavi A, Williams BA, McCue K et al (2008) Mapping and quantifying mammalian transcriptomes by RNA-Seq. *Nat Methods* 5:621–628. <https://doi.org/10.1038/nmeth.1226>
- Nawrocki WJ, Tourasse NJ, Taly A et al (2014) The plastid terminal oxidase: its elusive function points to multiple contributions to plastid physiology. *Annu Rev Plant Biol* 66:150112150216002. <https://doi.org/10.1146/annurev-arplant-043014-114744>
- Oshlack A, Wakefield M (2009) Transcript length bias in RNA-seq data confounds systems biology. *Biol Direct* 4:14. <https://doi.org/10.1186/1745-6150-4-14>
- Pankowski A, Mcminn A (2008) Iron availability regulates growth, photosynthesis, and production of ferredoxin and flavodoxin in Antarctic sea ice diatoms. *Aquat Biol* 4:273–288. <https://doi.org/10.3354/ab00116>
- Peers G, Price NM (2006) Copper-containing plastocyanin used for electron transport by an oceanic diatom. *Nature* 441:341–344. <https://doi.org/10.1038/nature04630>
- Peters E, Thomas DN (1996) Prolonged darkness and diatom mortality I: marine antarctic species. *J Exp Mar Bio Ecol* 207:25–41. [https://doi.org/10.1016/S0022-0981\(96\)02520-8](https://doi.org/10.1016/S0022-0981(96)02520-8)
- Petrou K, Trimborn S, Rost B et al (2014) The impact of iron limitation on the physiology of the Antarctic diatom *Chaetoceros* simplex. *Mar Biol* 161:925–937. <https://doi.org/10.1007/s00227-014-2392-z>
- Raven JA (1990) Predictions of Mn and Fe use efficiencies of photosynthetic growth as a function of light availability for growth and of C assimilation pathway. *New Phytol* 116:1–18. <https://doi.org/10.1111/j.1469-8137.1990.tb00505.x>
- Raven JA (2013) Iron acquisition and allocation in stramenopile algae. *J Exp Bot* 64:2119–2127. <https://doi.org/10.1093/jxb/ert121>
- Raven JA, Evans MCW, Korb RE (1999) The role of trace metals in photosynthetic electron transport in O₂-evolving

- organisms. *Photosynth Res* 60:111–149. <https://doi.org/10.1023/a:1006282714942>
- Richardson TL, Cullen JJ (1995) Changes in buoyancy and chemical composition during growth of a coastal marine diatom: ecological and biogeochemical consequences. *Mar Ecol Prog Ser* 128:77–90. <https://doi.org/10.3354/meps128077>
- Saba GK, Fraser WR, Saba VS et al (2014) Winter and spring controls on the summer food web of the coastal West Antarctic Peninsula. *Nature Comm* 5:4318. <https://doi.org/10.1038/ncomms12807>
- Sallée J-B, Speer KG, Rintoul SR (2010) Zonally asymmetric response of the Southern Ocean mixed-layer depth to the Southern Annular Mode. *Nat Geosci* 3:273–279. <https://doi.org/10.1038/ngeo812>
- Schrader PS, Milligan AJ, Behrenfeld MJ (2011) Surplus photosynthetic antennae complexes underlie diagnostics of iron limitation in a cyanobacterium. *PLoS ONE*. <https://doi.org/10.1371/journal.pone.0018753>
- Simão FA, Waterhouse RM, Ioannidis P et al (2015) BUSCO: assessing genome assembly and annotation completeness with single-copy orthologs. *Bioinformatics* 31:3210–3212. <https://doi.org/10.1093/bioinformatics/btv351>
- Smetacek V, Klaas C, Strass VH et al (2012) Deep carbon export from a Southern Ocean iron-fertilized diatom bloom. *Nature* 487:313–319. <https://doi.org/10.1038/nature11229>
- Smith WOJR, Ainley DG, Arrigo KR (2014) The oceanography and ecology of the Ross Sea. *Ann Rev Mar Sci* 6:469–487. <https://doi.org/10.1146/annurev-marine-010213-135114>
- Strzepek RF, Harrison PJ (2004) Photosynthetic architecture differs in coastal and oceanic diatoms. *Nature* 431:689–692. <https://doi.org/10.1038/nature02954>
- Strzepek RF, Maldonado MT, Hunter KA et al (2011) Adaptive strategies by Southern Ocean phytoplankton to lessen iron limitation: uptake of organically complexed iron and reduced cellular iron requirements. *Limnol Oceanogr* 56:1983–2002. <https://doi.org/10.4319/lo.2011.56.6.1983>
- Strzepek RF, Hunter KA, Frew RD et al (2012) Iron-light interactions differ in Southern Ocean phytoplankton. *Limnol Oceanogr* 57:1182–1200. <https://doi.org/10.4319/lo.2012.57.4.1182>
- Suggett DJ, Moore CM, Hickman AE, Geider RJ (2009) Interpretation of fast repetition rate (FRR) fluorescence: signatures of phytoplankton community structure versus physiological state. *Mar Ecol Prog Ser* 376:1–19. <https://doi.org/10.3354/meps07830>
- Sunda WG, Huntsman SA (1995) Iron uptake and growth limitation in oceanic and coastal phytoplankton. *Mar Chem* 50:189–206. [https://doi.org/10.1016/0304-4203\(95\)00035-P](https://doi.org/10.1016/0304-4203(95)00035-P)
- Sunda WG, Huntsman SA (1997) Interrelated influence of iron, light and cell size on marine phytoplankton growth. *Nature* 390:389–392. <https://doi.org/10.1038/37093>
- Timmermans KR, Davey MS, Van der Wagt B et al (2001) Co-limitation by iron and light of *Chaetoceros brevis*, *C. dictyota* and *C. calcitrans* (Bacillariophyceae). *Mar Ecol Prog Ser* 217:287–297. <https://doi.org/10.3354/meps217287>
- Timmermans KR, Van Der Wagt B, de Baar HJW (2004) Growth rates, half saturation constants, and silicate, nitrate, and phosphate depletion in relation to iron availability of four large open-ocean diatoms from the Southern Ocean. *Limnol Oceanogr* 49:2141–2151. <https://doi.org/10.4319/lo.2004.49.6.2141>
- van Oijen T, van Leeuwe MA, Gieskes WW, de Baar HJ (2004) Effects of iron limitation on photosynthesis and carbohydrate metabolism in the Antarctic diatom *Chaetoceros brevis* (Bacillariophyceae). *Eur J Phycol* 39:161–171. <https://doi.org/10.1080/0967026042000202127>
- Venables HJ, Clarke A, Meredith MP (2013) Wintertime controls on summer stratification and productivity at the western Antarctic Peninsula. *Limnol Oceanogr* 58:1035–1047. <https://doi.org/10.4319/lo.2013.58.3.1035>
- Yoshida K, Terashima I, Noguchi K (2007) Up-regulation of mitochondrial alternative oxidase concomitant with chloroplast over-reduction by excess light. *Plant Cell Physiol* 48:606–614. <https://doi.org/10.1093/pcp/pcm033>